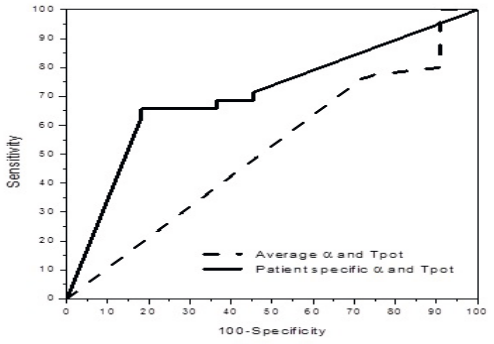

Figure 1. ROC curves for TCP calculated using either average (dashed line) or patient specific (solid line) parameters α and T_{pot}.

The dashed line corresponding to the TCP calculation based on average α and T_{pot} shows that the method has no power of discrimination with an area under the curve (AUC) of about 0.5. On the other hand, the ROC curve obtained based on patient specific α and T_{pot} (solid line) has an AUC of 0.7 and therefore this method does have an ability to distinguish between the two groups of patients presenting or not local control. The optimal threshold for TCP determined based on ROC analysis is 93% corresponding to a sensitivity of 66% and a specificity of 80%.
Conclusions: This study shows that individual radiobiological parameters used for modelling TCP are better predictors of the radiation treatment outcome in individuals than literature-based average parameters.

OC-0544
Dose distributions optimized to microscopic disease probability distribution in breast conserving therapy
W. Chen[1], J. Stroom[2], K. Gilhuijs[3], H. Bartelink[1], J.J. Sonke[1]
[1]*The Netherlands Cancer Institute - Antoni van Leeuwenhoek Hospital, Radiotherapy, Amsterdam, The Netherlands*
[2]*Champalimaud Foundation, Radiotherapy, Lisboa, Portugal*
[3]*University Medical Centre Utrecht, Radiology, Utrecht, The Netherlands*

Purpose/Objective: Residual microscopic disease (RMD) is considered to be the major cause of local recurrence in breast conserving therapy. Little knowledge, however, is available on how to optimally take the presence of RMD into consideration during radiotherapy. Traditionally, the whole breast is irradiated with/without a boost to the surgical bed. The purpose of this study was to optimize dose distributions to microscopic disease probability distribution obtained from detailed histopathology analyses.
Materials and Methods: Population statistics of RMD were derived from 1818histopathology slides of 60 breast-cancer patients. The absolute quantity was fitted to a Poisson model and the relative ratio of RMD distribution was modeled with a half-Gaussian curve. A simulation framework was proposed. For simplicity,we assume a unifocal spherical tumor surgically removed from the center of a half spherical breast of 14 cm diameter with 5mm isotropic surgical margins.Perfectly spherical dose distributions with a 3.2 mm penumbra width were considered,while ignoring setup error and organ motion. A modified Webb-Nahum tumour control probability (TCP) model was adopted with parameters optimized to the histopathology data and the event data from the EORTC boost-vs-no-boost trial (uniform 50 Gy with/without 16 Gy at tumour bed) and the fifth cycle study of EBCTCG. Non-uniform dose distributions were optimized with TCPs equivalent to a uniform dose distribution of 50 Gy with and without a 16 Gy boost to a 3 cm diameter PTV. To that end, 10000 virtual patients were sampled from the RMD probability distributions and the dose distributions were iteratively optimized by adding 1Gy at the radial distance with the largest TCP gain over the population of virtual patients.
Results: The RMD volume per patient approximates 140 mm^3on average and varies from 0 to 1076 mm^3. One standard deviation(SD) of the half-Gaussian model was 6.3 mm (Figure 1-1, R-square 0.93). The radiosensitivity of disease cells in the TCP model is estimated to be 0.056Gy^{-1} on average and with a Gaussian SD 0.009 Gy^{-1}. The optimal dose distributions have a maximum dose 88 Gy at 1 mm to the surgical bed and the minimum dose 0 Gy (Figure 1-2). Our TCP model characteristics are shown by the relation curve between uniform dose and TCP assuming patients with average disease volume (Figure 2-1). The DVH within 25 mm to the surgical bed illustrates the possible reduction of high dose volume by the proposed dose distributions (Figure 2-2).

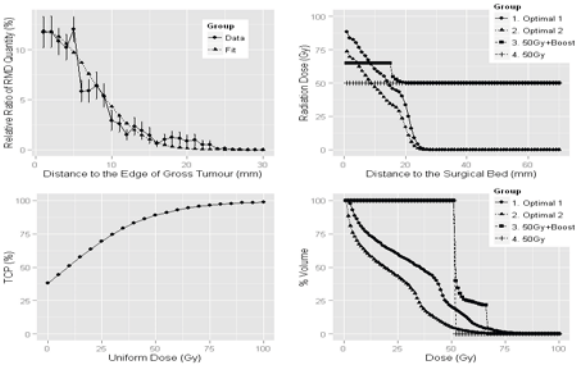

Conclusions: Using a detailed microscopic disease distribution from histopathology analyses, the radiation treatment on the operated breast can be further optimized. The proposed dose distribution keeps the overall TCP the same but may largely reduce the high-radiation dose volume compared to the conventional treatment.

OC-0545
Correlations between tumor oxygenation and FMISO PET data simulated based on microvasculature images
D. Moennich[1], E.G.C. Troost[2], J.H.A.M. Kaanders[3], W.J.G. Oyen[4], M. Alber[1], D. Zips[5], D. Thorwarth[1]
[1]*University Hospital Tübingen, Section for Biomedical Physics, Tübingen, Germany*
[2]*Maastricht University Medical Center, Department of Radiation Oncology (MAASTRO), Maastricht, The Netherlands*
[3]*Radboud University Nijmegen Medical Centre, Institute of Oncology - Radiation Oncology, Nijmegen, The Netherlands*
[4]*Radboud University Nijmegen Medical Centre, Institute of Oncology - Nuclear Medicine, Nijmegen, The Netherlands*
[5]*University Hospital Tübingen, Department of Radiation Oncology, Tübingen, Germany*

Purpose/Objective: Tumor hypoxia is associated with a poor outcome after radiotherapy. It can be assessed non-invasively by positron emission tomography (PET) using radiotracers that accumulate in poorly oxygenated tissue, such as ^{18}F-Fluoromisonidazole (FMISO). However, only moderate correlations were reported between FMISO PET and direct PO_2 measurements with oxygen sensing probes. Possible explanations were investigated in this study. Moreover, it was the purpose of this study to evaluate correlations between key figures of tumor oxygenation and different parameters that can be derived from FMISO PET imaging.
Materials and Methods: Tumor tissue oxygenation was computationally simulated based on microvasculature images obtained from immunohistochemically stained tissue sections. Subsequently, the corresponding distribution-retention dynamics of FMISO was simulated. Sets of O_2 and FMISO parameters were evaluated for 300 distinct vessel configurations. As oxygenation key figures of a voxel, the vital hypoxic fraction (vHF) and the meanPO_2 were chosen. For FMISO the PET voxel signal four hours after tracer injection (F_{4h}) and the ratio between F_{4h} and the mean signal during the first 15 min after injection ($F_{H/P}$) were used. A correlation analysis was performed. This was followed by a receiver operating characteristic (ROC) analysis of how effectively hypoxia can be identified based on F_{4h} and $F_{H/P}$.
Results: In hypoxic tissue F_{4h} is well correlated with vHF (R^2=0.90), while the correlation with meanPO_2 is low (R^2=0.22). A high nonlinear correlation was found between $F_{H/P}$ and meanPO_2 (R^2=0.99). The ROC analysis showed that tumor regions with a meanPO_2 below 2.5 mmHg can be identified with high sensitivity and specificity by applying an appropriate threshold to $F_{H/P}$ (YI=sensitivity+specificity-1=0.94). The accuracy of F_{4h} is considerably lower (YI=0.68). Both parameters are moderately effective in identifying critical PO_2 levels on the microscopic length-scale (YI=0.63 and 0.60).
Conclusions: A single static FMISO PET scan performed four hours after tracer injection appears to be suitable to estimate the vital hypoxic fraction in small tissue areas. A surrogate measure for the mean voxel PO_2 might be provided by incorporating supplementary information from a second static FMISO PET scan performed instantly after tracer administration. Clinical investigations have to show which parameter is better suited for predicting radiotherapy outcome and, in a further step, might be used to prescribe a hypoxia-specific dose.